

Structural basis for the presence of a monoglycosylated oligosaccharide in mature glycoproteins

Hyo-il Jung^a, Young Hwan Kim^b, Soohyun Kim^{c,*}

^a Department of Mechanical Engineering, Yonsei University, Seoul, Republic of Korea

^b Proteomics Team, Korea Basic Science Institute, Daejeon 305-333, Republic of Korea

^c Glycomics Team, Korea Basic Science Institute, Daejeon 305-333, Republic of Korea

Received 20 February 2005

Available online 30 March 2005

Abstract

Arylporin is an insect hexameric storage protein. The structures of the oligosaccharides attached to this protein have recently been determined. However, their precise functions remain to be established. Proteolysis and MALDI MS studies disclose that the amino acid residues Asn196 and Asn344 are *N*-glycosylated with Glc₁Man₉GlcNAc₂ and Man_{5–6}GlcNAc₂ oligosaccharides, respectively. Interestingly, significant variations in the amounts of glycans involving Glc₁Man₉GlcNAc₂ are evident in arylporins purified from larvae reared at different seasons. The data suggest that the metabolism of larvae and local protein structure contribute to glycan development. Three-dimensional model of the protein speculated that *N*-glycosidic linkage to Asn196 in the Glc₁Man₉GlcNAc₂ structure was buried inside the twofold axis of the hexamer, whereas oligosaccharide linkages to Asn344 were completely exposed to solvent. This finding is in agreement with previous biochemical data showing that limited Glc₁Man₉GlcNAc₂ was released by protein-*N*-glycosidase F under non-denaturing conditions, in contrast to Man_{5–6}GlcNAc₂ oligosaccharides.

© 2005 Elsevier Inc. All rights reserved.

Keywords: Insect; Arylporin; Hexamerin; Glycoprotein; Glycans; Monoglycosylated oligosaccharides; Homology modelling

Insect hexamerins belong to a growing superfamily of arthropod proteins that includes chelicerate and crustacean hemocyanins [1], arthropod tyrosinases [2,3], and the dipteran hexamerin receptors [4,5]. Despite clear structural similarities, these proteins serve very different functions. Hemocyanins form hexamers or multihexamers of identical or closely related subunits, and carry oxygen in the hemolymph of arthropods by virtue of two copper ions bound per monomer [6]. Insect hexamerins also form hexamers, but with no ability to bind copper ions, and consequently, oxygen. It is proposed that hexamerins have evolved from hemocyanins of ancient crustaceans [1,5], in view of the proposed sister group position of these subphyla [7–9].

Hexamerins are synthesized from the fat body of a wide range of lepidopteran and dipteran larvae, among other insect orders. These proteins are accumulated to high concentrations in the hemolymph. Hexamerins appear to be the central source of a storage pool of amino acid resources for complete development of the adult, since insect pupae do not feed during metamorphosis. There are at least two types of hexamerins in lepidoptera. These form loose clusters on a bivariate plot of the proportion of aromatic amino acids (tyrosine plus phenylalanine) versus methionine [10]. One is arylporin that is rich in aromatic amino acids, while the second is a methionine-rich storage protein. All the proteins are hexamers composed of approximately 80 kDa subunits, leading to molecular masses at around 500 kDa [10].

The Chinese oak silkworm, *Antherea pernyi*, is a lepidoptera, along with the economically important wild

* Corresponding author. Fax: +82 42 865 3419.

E-mail address: shkim@kbsi.re.kr (S. Kim).

silkmoth found in Europe and Far Eastern Asia. We previously described the oligosaccharide structures and possible functions of *A. pernyi* arylphorin [11]. Unexpectedly, arylphorin mainly contains the monoglycosylated oligosaccharide, Glc₁Man₉GlcNAc₂, in the glycan pool, as well as simple oligomannose and truncated oligosaccharides.

Among the hemolymph proteins of *A. pernyi*, Glc₁Man₉GlcNAc₂ oligosaccharides are only associated with arylphorin, and are not released from the native protein by protein-*N*-glycosidase (PNGase) F treatment, in contrast to Man_{5–6}GlcNAc₂ and paucimannose glycans [11]. Accordingly, it is speculated that the *N*-glycosidic linkage to Glc₁Man₉GlcNAc₂ is buried in the hexamer, while the other oligosaccharides are exposed on the surface of the protein. Here we identify the glycosylation sites by proteolysis and matrix-assisted laser desorption/ionization time-of-flight (MALDI-TOF) mass spectrometric analysis, and report a three-dimensional structure of arylphorin hexamer by homology modelling. This structural information should shed light on the role of sugars in the folding and assembly of macromolecular glycoproteins, such as arylphorin.

Materials and methods

Materials. Materials were obtained from Sigma Chemical (St. Louis, Missouri, USA), except HPLC solvents, which were purchased from Fisher. Exoglycosidases and PNGase F were purchased from Prozyme (San Leandro, CA, USA) and New England Biolabs (Beverly, MA, USA), respectively. The Chinese oak silkworm, *A. pernyi*, was raised twice a year (late spring and autumn) in the oak tree field established in Miryang National University, Korea. Larvae of *A. pernyi* were reared on fresh or freezer-stored mulberry leaves.

Hemolymph collection. The abdominal leg of the silkworm at the fifth larval stage was injured with sharpened scissors, and hemolymph bled from the wound. Hemolymph was directly collected into pre-cooled test tubes with a few crystals of 1-phenyl-2-thiourea to inhibit phenol oxidase. Next, hemolymph was centrifuged at 5000g for 15 min to remove hemocytes and other debris. Prepared hemolymph was maintained at –70 °C until analysis.

Purification of arylphorin. Arylphorin was separated by gel filtration on a Superdex pg 200 column (16 × 60 cm, Pharmacia, Uppsala, Sweden), as described previously [11]. The buffer employed was 50 mM sodium phosphate, pH 7.5, containing 0.1 M sodium chloride. The flow rate was 1.0 ml/min, and eluting proteins were monitored at 280 nm. Arylphorin was eluted immediately after the void volume of the column.

Preparation and analysis of arylphorin glycopeptides. Purified arylphorin (10 µg) was denatured and digested with trypsin, as described elsewhere [12]. The reaction was terminated by heating for 2 min at 100 °C and diluted with 20 volumes of buffer A (10 mM Tris, 150 mM NaCl, 1 mM CaCl₂, and 1 mM MnCl₂, pH 7.5). The mixture was applied to 0.3 ml Con A-Sepharose (Amersham Pharmacia, Uppsala, Sweden) packed into a mini-column (Bio-Rad, Hercules, CA), equilibrated with the buffer, and washed with six volumes of binding buffer A. Glycopeptides were eluted twice with 1 ml of the above buffer containing 100 mM α-methyl-mannoside. Effluents were pooled and applied to 0.3 ml of the mini-C18 column equilibrated with methanol and water. Salts and sugars were removed by washing the column with

3 ml water, and glycopeptides were eluted with 1 ml of 50% methanol. Glycopeptides were lyophilized and stored at –20 °C until analysis.

Oligosaccharide preparation and analysis. Arylphorins (10 µg) were employed for glycan analysis. Oligosaccharide release from proteins, 2-aminobenzamide labelling of glycans, and separation by normal-phase HPLC were carried out as described previously [11].

Identification of glycosylation sites. N-glycosylation sites in arylphorin were initially predicted with the NetNGlyc server [<http://www.cbs.dtu.dk/services/NetNGlyc/>] using artificial neural networks that examine the context of Asn-Xaa-Ser/Thr sequences [13]. To establish the site of N-glycosylation on the protein, MALDI-TOF mass spectrometry (MS) was used. All mass spectra were recorded on Voyager DE-STR (ABI) MALDI-TOF MS in the positive linear mode at 20 kV accelerating voltage. All samples were irradiated with UV light (337 nm) from the N₂ laser at a repetition rate of 3 Hz and average of 500 laser shots. Mass spectra were externally calibrated using a standard peptide mixture that was spotted adjacent to the sample spot. The 2,5-dihydroxybenzoic acid (DHB) matrix was prepared by dissolving 10 mg DHB in 1 ml acetonitrile/water (1:1, v/v). 0.5 µl of sample dissolved in deionized water (20 µl) was loaded on the MALDI target and mixed with 0.5 µl DHB matrix solution. Sample spots were allowed to dry at room temperature and re-dissolved in 0.1 µl ethanol for re-crystallization.

Modelling of oligosaccharides. Three-dimensional atomic coordinates of oligosaccharides were obtained from the glycosciences database SWEET-DB [14] [<http://www.dkfz-heidelberg.de/spec2/sweetdb/>] in which spatial representations were generated with SWEET-II [15] and optimized using the MM3 force field, as implemented in the TINKER molecular modelling package [16]. Oligosaccharide structures were obtained with the graphical software, PyMOL (<http://pymol.sourceforge.net/>).

Sequence alignment and homology modelling of arylphorin. The amino acid sequence of the Chinese oak silkworm *A. pernyi* arylphorin (704 residues), was obtained from the Swiss-Prot/TrEMBL protein database (Accession No. AAP34685). Highly homologous sequences with known three-dimensional structures were identified from a sequence-structure homology recognition program, FUGUE [<http://www-cryst.bioc.cam.ac.uk/fugue/>] [17]. The resulting sequences were aligned and formatted using JOY [18].

Three-dimensional models of the arylphorin monomer were generated using the MODELLER package [<http://www.salilab.org/modeller/modeller.html>] [19]. Models were based on the crystal structures of hemocyanin proteins from *Panularus interruptus* (3.20 Å, 1hc1-6) and *Limulus polyphemus* (2.20 Å, 1lla) available within the Protein Data Bank. The quality of the protein model was evaluated with two different validation programs, specifically, Verify3D [20] and RAM-PAGE [21].

Results and discussion

Identification of glycosylation sites

Asn57, Asn196, and Asn344 of arylphorin are *N*-glycosylated, as predicted using the NetNGlyc 1.0 Server (<http://www.cbs.dtu.dk/services/NetNGlyc/>). To determine the glycosylation site and glycoform at each site, the glycopeptide pool was subjected to MALDI-TOF MS analysis. MS signals disclosed two *N*-glycosylation sites in arylphorin, specifically, Asn196 and Asn344 (Fig. 1). These include oligomannose and truncated glycans with or without fucosylation, in agreement with a previous study [11]. The biggest structure detected was consistent with the assignment of Glc₁Man₉GlcNAc₂.

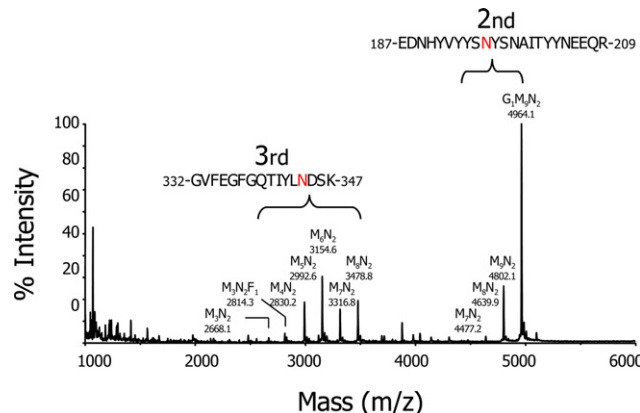


Fig. 1. Glycosylation site analysis of arylphorin by MALDI MS. Glycopeptides were prepared as described in Materials and methods. All molecular weights represent the monoisotopic masses of the respective $[M + Na]^+$ ions of a particular glycan species. The major structures are depicted as follows: G, glucose; M, mannose; N, N-acetylglucosamine; and F, fucose.

Interestingly, the second site was occupied by bigger oligomannose structures, including monoglucosylated glycan, which were processed to a limited extent in ER. However, the third site mainly contained $Man_{5-6}GlcNAc_2$ which were mostly processed glycans and the same ones obtained as native arylphorin was treated with PNGase F [11]. The data collectively indicate that the second N-glycosylation site is in a restricted local structure for processing glycosidases (such as α -glucosidase II or α -mannosidase), while the third site is in a freely accessible location.

Seasonal variation of the glycan profile

Protein glycosylation is significantly affected by environmental conditions, including temperature and food. *A. pernyi* larvae are cultured twice a year, specifically, in the spring and autumn. Arylphorin purified from larvae reared during the spring contains both truncated and simple oligomannose type glycans, including monoglucosylated oligosaccharide (Fig. 2A). In contrast, the storage protein of larvae grown in the autumn mainly contains monoglucosylated oligosaccharide, along with oligomannose type glycans (Fig. 2B). The findings suggest that development of the oligosaccharide structure is dependent on the metabolic rate of a given organism. Additionally, the local protein structure of arylphorin may affect glycan processing, since monoglucosylated oligosaccharide is universally present in proteins which are extracted from larvae reared at different seasons. We conclude from the data that de-glucosylation at the second glycosylation site is not completed before the end of appropriate protein folding and assembly, so monoglucosylated oligosaccharide remained in the mature protein.

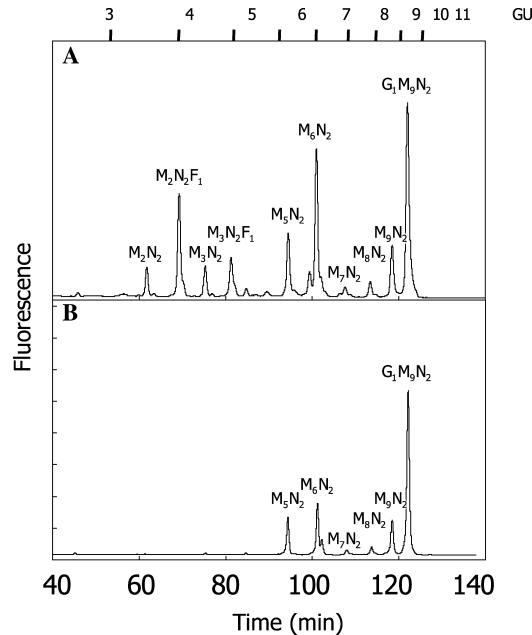


Fig. 2. Seasonal variation of the glycan profile released from *A. pernyi* arylphorin. Oligosaccharide preparation and analysis are described in Materials and methods. Arylphorin glycans were obtained from larvae grown in the (A) spring or (B) autumn. Oligosaccharide structures are described as follows: G, glucose; M, mannose; N, N-acetylglucosamine; and F, fucose.

Sequence alignment of the arylphorin monomer

To determine the glycosylation sites in a three-dimensional conformation of arylphorin, homology modelling was performed. Two hemocyanin proteins (*P. interruptus* and *L. polyphemus*) were selected as the templates. The overall sequence identity between arylphorin and hemocyanin was 28%. However, when structurally related amino acid residues in the mismatch positions were included, the sequence similarity increased up to 45%. Using the program FUGUE, the amino acid sequence of arylphorin (residues 17–665) was aligned with those of hemocyanin monomers from *P. interruptus* (residues 5–653) and *L. polyphemus* (residues 2–628), whose crystal structures have been solved at resolutions of 3.2 Å [23] and 2.0 Å [24], respectively (Fig. 3). A Z-score of 88.13 was calculated from the alignment. The data indicate that the arylphorin monomer contains 16 α -helices, 3 β -strands, and 15 β -strands.

Homology modelling of the arylphorin hexamer

The insect storage protein, arylphorin, consists of six homogeneous subunits [10]. The structure of the arylphorin monomer was obtained using the program MODELLER (Fig. 4A), and the hexamer was constructed based on the atomic coordinates of hemocyanin protein chains A to F (*P. interruptus*) (Fig. 4B). The model structure of the arylphorin monomer was

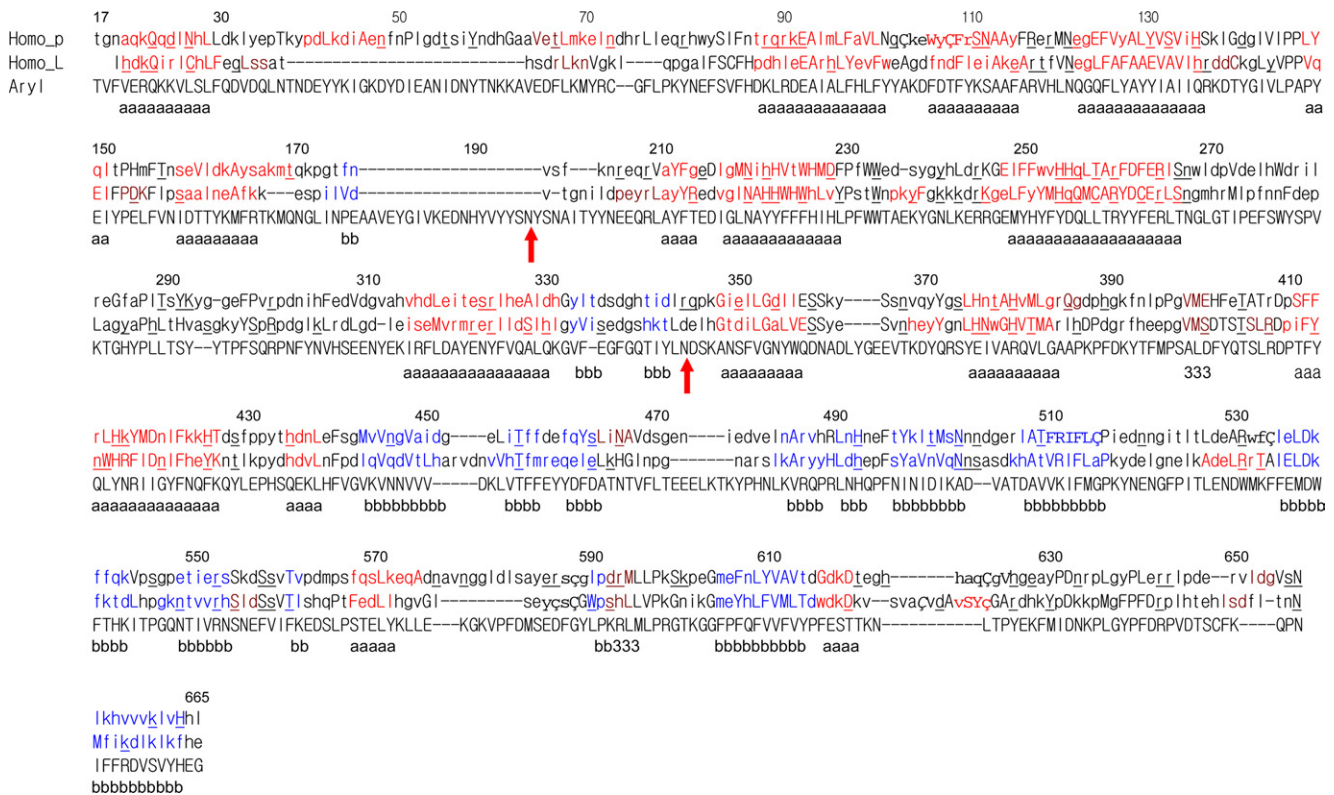


Fig. 3. Sequence alignment of arylphorin with hemocyanin proteins of *P. interruptus* and *L. polyphemus*. Lowercase, solvent accessible; uppercase, solvent inaccessible; bold, hydrogen bond to main-chain amide; underline, hydrogen bond to main-chain carbonyl; cedilla, disulfide bond; and italic, positive ϕ torsion angle. The proposed secondary structure elements in the arylphorin structure are specified (a, α -helix; b, β -strand; and 3, 3_{10} -helix). Glycosylated Asn residues are indicated with arrows. Aryl, arylphorin; Hemo_P, *P. interruptus* hemocyanin; and Hemo_L, *L. polyphemus*.

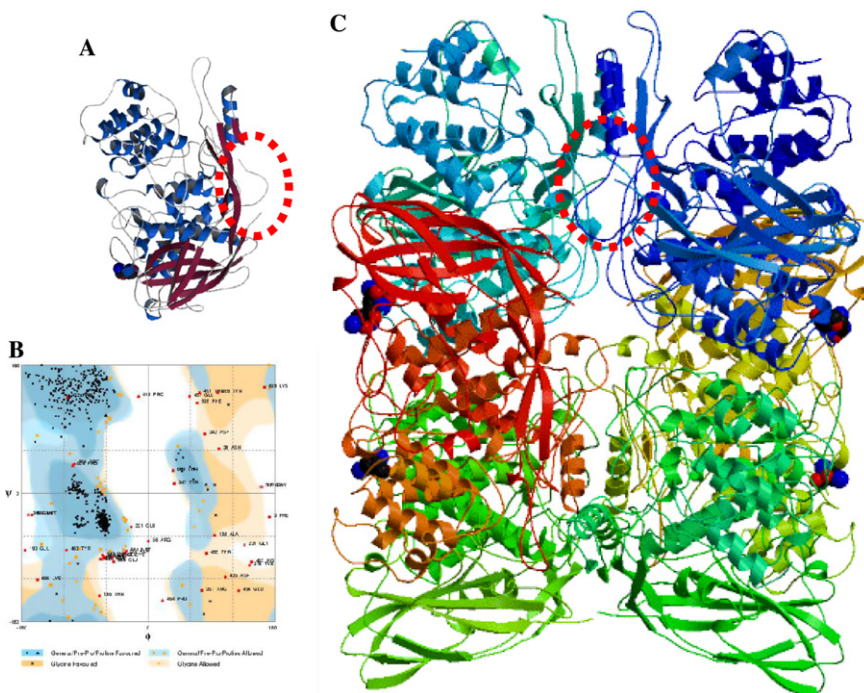


Fig. 4. Molscript [22] representation of homology-modelled structures of arylphorin monomer and hexamer. (A) Cartoon representation of the predicted *A. pernyi* monomer structure. The potential second glycosylation residue is depicted with dotted open circles, and the Asn residue of the third site as spheres. (B) Hexameric structure of arylphorin. The view represents the twofold axis of the hexamer. (C) Ramachandran plot of the model structure of the monomer. The total number of residues analyzed is 626. The graph was prepared using the program RAMPAGE [25].

analyzed using the validation software, RAMPAGE [21], to evaluate its stereochemical quality. A Ramachandran plot exhibited good distribution for the $[\phi]/[\psi]$ angles, consistent with a good quality model (Fig. 4C). For the monomer, 85.1% (533) of residues (non-Gly and non-Pro) were in the most favored regions,

7.8% (49) in the additionally allowed regions, and 7.0% (44) in the disallowed regions. The model was further validated with the program Verify3D [20]. Each monomer scored between 0.00 and 0.82 (versus between 0.12 and 0.72 for *P. interruptus*, and 0.05 and 0.69 for *L. polyphemus*).

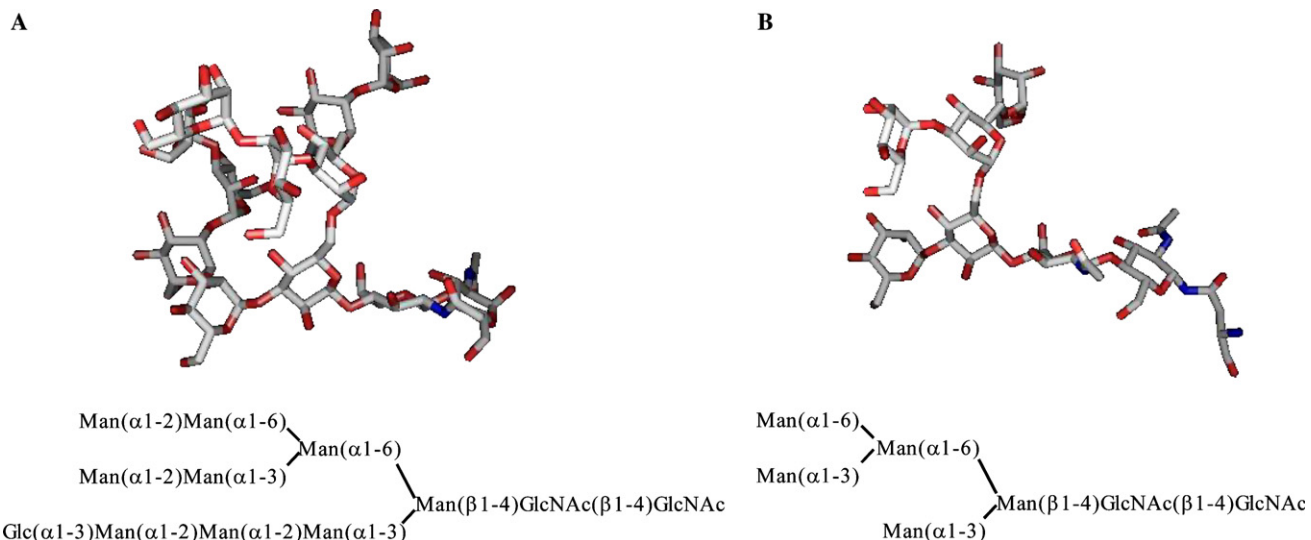


Fig. 5. The three-dimensional model structures of glycans. Atomic coordinates were obtained from a carbohydrate-related database (SWEET-DB: <http://www.dkfz-heidelberg.de/spec2/sweetdb/>) [14]. A graphical presentation was prepared using the software PyMol (<http://pymol.sourceforge.net/>).

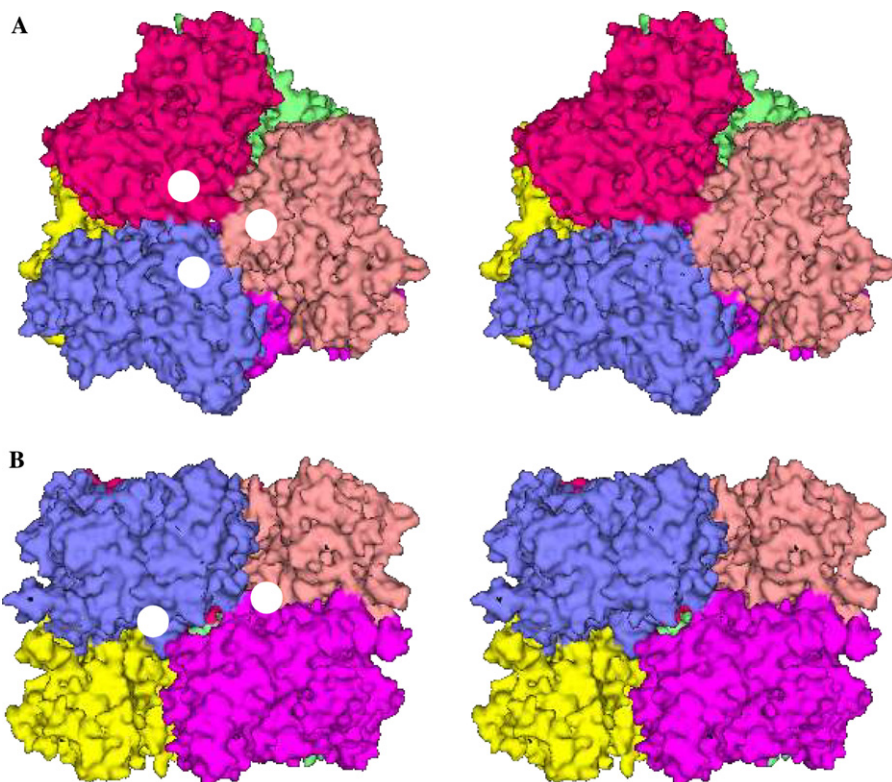


Fig. 6. Stereo view of the arylphorin hexamer. The molecular surface of the arylphorin hexamer is illustrated using the graphical software, PyMol. (A) Orthogonal view of the hexamer; (B) side view of the hexamer. Potential glycosylation sites are depicted as closed circles.

Molecular modelling of arylphorin

The sequence alignment (Fig. 3) revealed no consensus sequence within arylphorin between Tyr194 and Phe213, which contains the second monoglycosylated oligosaccharide site. It was almost impossible to build up a reliable structure by current computer-aided modelling technologies due to lack of homology, particularly in situations where a number of sequences (i.e., 20 amino acids) were missing. Although the missing sequences contain the second glycosylation site, it was possible to identify this site with the help of neighboring sequences. In this regard, the homology model structure was built up with truncated sequences from 194 to 213. According to the model structure, amino acids 194–213 are buried in the twofold axis of the hexamer (Figs. 4B and 6B). Therefore, Asn196 of the second glycosylation site is unlikely to be exposed to the surface of the protein hexamer, and the *N*-glycosidic linkage of this residue is completely buried inside the protein. However, the three-dimensional structure of the monoglycosylated glycan is bulky, as shown in Fig. 5. We thus speculate that the bulky structure protrudes outside the interface of the two trimers due to steric hindrance (Fig. 6B).

While the precise conformation of the Glc₁Man₉GlcNAc₂ oligosaccharide is yet to be determined, it is clear that Asn196 of the second glycosylation site is inaccessible consistent with previous biochemical data [11]. In contrast, Asn344 is located on the surface of the protein hexamer, implying that the third glycosylation site is fully exposed to solvent (Figs. 4A and 6A). PNGase F treatment of native or denatured arylphorin released simple oligomannose type glycans [11] typically present in the third site.

Glc₁Man₉GlcNAc₂ is rarely identified in native mature glycoproteins, but has been described in many species. A wide range of storage proteins, such as immunoglobulins of egg yolk of hen, Japanese quail or pigeon [26–28] or tissues, such as egg jelly coat of a starfish, *Asterias amurensis*, and vitellogenetic substances from the ovary of *A. rubens* [29,30] and decapod crustacean *Cherax quadricarinatus* [31] contain the oligosaccharide as a major *N*-glycan. Moreover, monoglycosylated oligomannose comprises some 20–40% of the total glycans in α -mannosidase extracted from jack bean that is a plant storage tissue [32]. These are all large hydrophobic proteins. Khalaila et al. [31] suggested that protein size and hydrophobicity are linked to the presence of the monoglycosylated oligosaccharide, Glc₁Man₉GlcNAc₂. This is the first report on sterical resolution of the glycosylation site of arylphorin containing monoglycosylated oligosaccharide.

The crystal structure of the arylphorin hexamer is essential to locate glycans and establish their role in protein folding or assembly. The three-dimensional model reported in this study provides a starting point for addressing glycan function in arylphorin.

Acknowledgments

This work was supported by a grant, R01-2002-000-00224-0 (to S.K.), from the Basic Research Program and National Core Research Center for Nanomedical Technology Center (to H.J.) of the Korea Science and Engineering Foundation. The authors thank K.I. Kim for excellent MS operation and Dr. S.M. Lee for generously supplying larval hemolymph.

References

- [1] J.J. Beintema, W.T. Stam, B. Hazes, M.P. Smidt, Evolution of arthropod hemocyanins and insect storage proteins (hexamerins), *Mol. Biol. Evol.* 11 (1994) 493–503.
- [2] K. Fujimoto, N. Okino, S. Kawabata, S. Iwanaga, E. Ohnishi, Nucleotide sequence of the cDNA encoding the proenzyme of phenol oxidase A1 of *Drosophila melanogaster*, *Proc. Natl. Acad. Sci. USA* 92 (1995) 7769–7773.
- [3] T. Kawabata, Y. Yasuhara, M. Ochiai, S. Matsuura, M. Ashida, Molecular cloning of insect pro-phenol oxidase: a copper-containing protein homologous to arthropod hemocyanin, *Proc. Natl. Acad. Sci. USA* 92 (1995) 7774–7778.
- [4] T. Burmester, K. Scheller, Complete cDNA-sequence of the receptor responsible for arylphorin uptake by the larval fat body of the blowfly, *Calliphora vicina*, *Insect Biochem. Mol. Biol.* 25 (1995) 981–989.
- [5] T. Burmester, K. Scheller, Common origin of arthropod tyrosinase, arthropod hemocyanin, insect hexamerin, and dipteran arylphorin receptor, *J. Mol. Evol.* 42 (1996) 713–728.
- [6] K.E. van Holde, K.I. Miller, Hemocyanins, *Adv. Protein Chem.* 47 (1995) 1–81.
- [7] J.M. Turbeville, D.M. Pfeifer, K.G. Field, R.A. Raff, The phylogenetic status of arthropods, as inferred from 18S rRNA sequences, *Mol. Biol. Evol.* 8 (1991) 669–686.
- [8] M. Averof, M. Akam, Insect–crustacean relationships: insights from comparative developmental and molecular studies, *Philos. Trans. R. Soc. Lond. B* 347 (1995) 293–303.
- [9] M. Friedrich, D. Tautz, Ribosomal DNA phylogeny of the major extant arthropod classes and the evolution of myriapods, *Nature* 376 (1995) 165–167.
- [10] W.H. Telfer, J.G. Kunkel, The function and evolution of insect storage hexamers, *Annu. Rev. Entomol.* 36 (1991) 205–228.
- [11] S. Kim, S.K. Hwang, R.A. Dwek, P.M. Rudd, Y.H. Ahn, E.H. Kim, C. Cheong, S.I. Kim, N.S. Park, S.M. Lee, Structural determination of the *N*-glycans of a lepidopteran arylphorin reveals the presence of a monoglycosylated oligosaccharide in the storage protein, *Glycobiology* 13 (2003) 147–157.
- [12] S.I. Kim, S.M. Kweon, E.A. Kim, J.Y. Kim, S. Kim, J.S. Yoo, Y.M. Park, Characterization of RNase-like major storage protein from the ginseng root by proteomic approach, *J. Plant Physiol.* 161 (2004) 837–845.
- [13] N. Blom, T. Sicheritz-Ponten, R. Gupta, S. Gammeltoft, S. Brunak, Prediction of post-translational glycosylation and phosphorylation of proteins from the amino acid sequence, *Proteomics* 4 (2004) 1633–1649.
- [14] A. Loss, P. Bunsmann, A. Bohne, A. Loss, E. Schwarzer, E. Lang, C.W. von der Lieth, SWEET-DB: an attempt to create annotated data collections for carbohydrates, *Nucleic Acids Res.* 30 (2002) 405–408.
- [15] A. Bohne, E. Lang, C.W. von der Lieth, W3-SWEET: carbohydrate modelling by Internet, *J. Mol. Model.* 4 (1998) 33–43.

- [16] R. Pappu, R. Hart, J. Ponder, Analysis and application of potential energy smoothing for global optimization, *J. Phys. Chem. B* 102 (1998) 9725–9742.
- [17] J. Shi, T.L. Blundell, K. Mizuguchi, FUGUE: sequence-structure homology recognition using environment-specific substitution tables and structure-dependent gap penalties, *J. Mol. Biol.* 310 (2001) 243–257.
- [18] K. Mizuguchi, C.M. Deane, T.L. Blundell, M.S. Johnson, J.P. Overington, JOY: protein sequence-structure representation and analysis, *Bioinformatics* 14 (1998) 617–623.
- [19] A. Sali, T.L. Blundell, Comparative protein modelling by satisfaction of spatial restraints, *J. Mol. Biol.* 234 (1993) 779–815.
- [20] R. Luthy, J.U. Bowie, D. Eisenberg, Assessment of protein models with three-dimensional profiles, *Nature* 356 (1992) 83–85.
- [21] S.C. Lovell, I.W. Davis, W.B. Arendall III, P.I.W. de Bakker, J.M. Word, M.G. Prisant, J.S. Richardson, D.C. Richardson, Structure validation by Calpha geometry: phi, psi and Cbeta deviation, *Proteins: Struct. Funct. Genet.* 50 (2002) 437–450.
- [22] P. Kraulis, MOLSCRIPT: a program to produce both detailed and schematic plots of protein structures, *J. Appl. Crystallogr.* 24 (1991) 946–950.
- [23] A. Volbeda, W.G. Hol, Crystal structure of hexameric haemocyanin from *Panulirus interruptus* refined at 3.2 Å resolution, *J. Mol. Biol.* 209 (1989) 249–279.
- [24] B. Hazes, K.A. Magnus, C. Bonaventura, J. Bonaventura, Z. Dauter, K.H. Kalk, W.G. Hol, Crystal structure of deoxygenated *Limulus polyphemus* subunit II hemocyanin at 2.18 Å resolution: clues for a mechanism for allosteric regulation, *Protein Sci.* 2 (1993) 597–619.
- [25] R.A. Laskowski, M.W. MacArthur, D.S. Moss, J.M. Thornton, PROCHECK—a program to check the stereochemical quality of protein structures, *J. Appl. Crystallogr.* 26 (1993) 283–291.
- [26] M. Ohta, J. Hamako, S. Yamamoto, H. Hatta, M. Kim, T. Yamamoto, S. Oka, T. Mizuuchi, F. Matsuura, Structures of asparagine-linked oligosaccharides from hen egg-yolk antibody (IgY). Occurrence of unusual glycosylated oligo-mannose type oligosaccharides in a mature glycoprotein, *Glycoconj. J.* 8 (1991) 400–413.
- [27] F. Matsuura, M. Ohta, K. Murakami, Y. Matsuki, Structures of asparagine linked oligosaccharides of immunoglobulins (IgY) isolated from egg-yolk of Japanese quail, *Glycoconj. J.* 10 (1993) 202–213.
- [28] N. Suzuki, K.-H. Khoo, C.-M. Chen, H.-C. Chen, Y.C. Lee, N-Glycan structures of pigeon IgG: a major serum glycoprotein containing Gall-4Gal termini, *J. Biol. Chem.* 278 (2003) 46293–46306.
- [29] T. Endo, M. Hoshi, S. Endo, Y. Arata, A. Kobata, Structures of the sugar chains of a major glycoprotein present in the egg jelly coat of a starfish, *Asterias amurensis*, *Arch. Biochem. Biophys.* 252 (1987) 105–112.
- [30] P. De Waard, J.P. Kamerling, H. Van Halbeek, J.F. Vliegenthart, J.J. Broertjes, Characterization of N-linked gluco-oligomannose type of carbohydrate chains of glycoproteins from the ovary of the starfish *Asterias rubens* (L.), *Eur. J. Biochem.* 168 (1987) 679–685.
- [31] I. Khalaila, J. Peter-Katalinic, C. Tsang, C.M. Radcliffe, E.D. Aflalo, D.J. Harvey, R.A. Dwek, P.M. Rudd, A. Sagi, Structural characterization of the N-glycan moiety and site of glycosylation in vitellogenin from the decapod crustacean *Cherax quadricarinatus*, *Glycobiology* 14 (2004) 767–774.
- [32] Y. Kimura, D. Hess, A. Sturm, The N-glycans of Jack bean α -mannosidase. Structure, topology and function, *Eur. J. Biochem.* 264 (1999) 168–175.